Persistence of Gulf Stream separation during the Last Glacial Period: Implications for current separation theories

Katsumi Matsumoto[1] and Jean Lynch-Stieglitz

Lamont-Doherty Earth Observatory of Columbia University, Palisades, New York, USA

Received 6 March 2001; revised 23 May 2002; accepted 17 December 2002; published 4 June 2003.

[1] We present stable oxygen isotope ratio ($\delta^{18}O$) measurements on deep-dwelling planktonic foraminifera from the western margin of the North Atlantic in order to reconstruct the latitude at which the Gulf Stream separated from the western boundary of the Atlantic Ocean in the past. The modern separation latitude can be reconstructed within one degree from $\delta^{18}O$ measured on the fossil shells of deep-dwelling planktonic foraminifera *Globorotalia truncatulinoides* from the Holocene sediments representing the past 10,000 years of mild climate conditions similar to today. The separation latitude is captured in a sharp $\delta^{18}O$ gradient, which reflects the prominent hydrographic change across the boundary between the warm waters south and east of the Gulf Stream and the cold Slope Water to the north. The latitudinal $\delta^{18}O$ profile from approximately the Last Glacial Maximum shows that the Gulf Stream separated from the coast near Cape Hatteras at almost the same latitude as it does today. We assess our finding in light of existing Gulf Stream separation theories and conclude that one of the theories, the wind-induced separation mechanism, is not consistent with our paleoceanographic reconstruction. *INDEX TERMS:* 4267 Oceanography: General: Paleoceanography; 4576 Oceanography: Physical: Western boundary currents; 4870 Oceanography: Biological and Chemical: Stable isotopes; 9325 Information Related to Geographic Region: Atlantic Ocean; *KEYWORDS:* Gulf Stream separation, western boundary current, planktonic foraminifera, oxygen isotope composition, Last Glacial Maximum, marine sediment cores

Citation: Matsumoto, K., and J. Lynch-Stieglitz, Persistence of Gulf Stream separation during the Last Glacial Period: Implications for current separation theories, *J. Geophys. Res.*, *108*(C6), 3174, doi:10.1029/2001JC000861, 2003.

1. Introduction

[2] The Gulf Stream is perhaps the dominant surface current in the North Atlantic (Figure 1), and its basic path has been known since the eighteenth century when merchant ships exploited its fast flow to quickly transport goods between Europe and its American colonies. Because the Gulf Stream is an important agent of poleward heat transport and is associated with large ocean-atmosphere heat flux, any change in its path may have significant regional climatic impacts. In addition, the Gulf Stream path impacts the economy through its control on fish stocks [*Myers and Drinkwater*, 1989].

[3] After leaving the Florida Straits, the Gulf Stream flows along the U. S. coastline following the continental slope between the shallow coastal area (~100 m) and the deeper region of Blake Plateau (~800 m) until reaching Cape Hatteras, located near 36°N. At this point, the western boundary current separates from the coast and travels northeast as freely meandering jet in the open ocean. On a basin-wide scale, the Gulf Stream separation latitude apparently changed very little over the recent decades. A 12-year observation between 1977 and 1988 shows that the separation near Cape Hatteras has been fixed to a meridional distance of ±50 km [*Gangopadhyay et al.*, 1992]. A compilation of the Gulf Stream position over a longer 30-year period between 1966 and 1996 at 72°W, near the point of separation, likewise shows that the latitudinal variability of the Gulf Stream is limited to less than a degree. In contrast, the variability of the meandering Gulf Stream after separation is significantly larger [*Taylor and Stephens*, 1998].

[4] Despite efforts to understand the Gulf Stream for more than 200 years since the time of Benjamin Franklin [*Franklin*, 1786], the Gulf Stream separation is not well understood dynamically nor is it reliably simulated in most ocean circulation models. In many models, irrespective of their spatial resolution, the Gulf Stream remains attached to the continental shelf all the way to Grand Banks, filling the region northeast of Cape Hatteras with warm subtropical water and exaggerating the ocean-to-atmosphere heat flux predictions there. In a recent review, *Dengg et al.* [1996] classify current theories of the Gulf Stream separation into six categories: (1) wind-forced separation; (2) inertial overshooting; (3) topographic effects; (4) detachment due to dynamically forced outcropping of isopycnal surfaces; (5)

[1]Now at Geological Survey of Japan, AIST Site 7, Tsukuba, Ibaraki, Japan.

0148-0227/03/2001JC000861$09.00

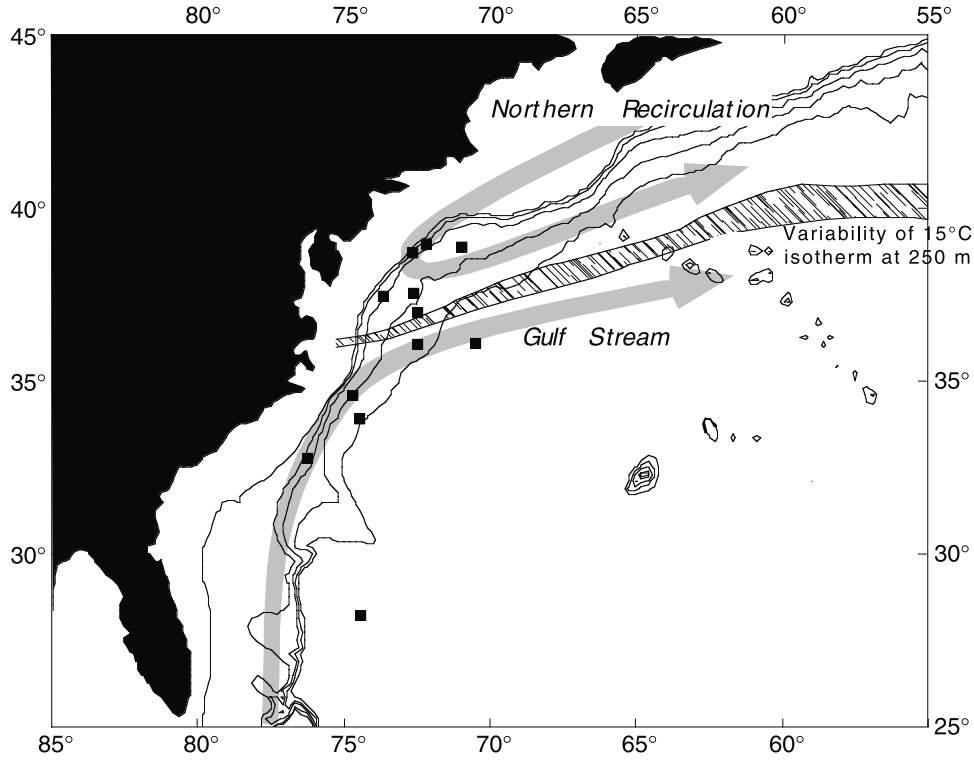

Figure 1. Regional setting and core sites (solid squares). Bathymetric contours of 500, 1000, 2000, 3000, and 4000 m are indicated by solid lines. The position of the 15°C isotherm at 250 m water depth migrates seasonally as indicated by the width of hatched lines. The 15°C isotherm serves as a boundary between the warm Sargasso Seawaters to the south and the cold Slope Water to the north. The point of Gulf Stream separation from the margin near Cape Hatteras is indicated by the intersection of the 15°C isotherm and bathymetric contours at around 36.5°N.

vorticity crisis; and (6) the joint effect of baroclinicity and relief. They note that many of these theories are only applicable under idealized dynamical conditions and do not provide enough clues to explain why models are unable to make better predictions.

[5] In this paper, we evaluate these separation theories by reconstructing the Gulf Stream separation during approximately the Last Glacial Maximum (LGM, about 21,000 years ago) on the basis of stable oxygen isotope ratios ($\delta^{18}O$) measurements on deep-dwelling planktonic foraminifera. Plankton tow and culture studies have shown that planktonic foraminiferal calcite $\delta^{18}O$ reflects the temperature and salinity of the ambient seawater in which they calcifies [*Fairbanks et al.*, 1982; *Bemis et al.*, 1998]. A meridional transect of $\delta^{18}O$ measurements along the continental slope can identify the latitude of Gulf Stream separation as a sharp $\delta^{18}O$ gradient, which coincides with what Bache, who began the modern survey of the Gulf Stream in the mid-nineteenth century and was the grandson of Benjamin Franklin, called the "Cold Wall" [*Stommel*, 1950] that separates the warm Sargasso Seawater to the south and the cold Slope Water to the north.

[6] A major challenge of this study is obtaining adequate sediment materials with sufficient temporal constraint in the geologically complex western margin of the North Atlantic, where slumps and turbidity currents are common on the continental margin [*Horn et al.*, 1971; *Stanley et al.*, 1971]. In addition, the availability of foraminiferal tests is often minimal in glacial sediments, which are characterized by very low carbonate content [*Balsam*, 1981]. In this study, we used what appeared to us to be the most promising sediment cores available from the Lamont-Doherty Earth Observatory core repository, but we anticipate that spatial coverage and temporal constraint can be improved with new and larger sediment samples. For this reason, our glacial reconstruction of the Gulf Stream separation may be considered tentative.

2. Materials and Methods

[7] After an initial examination of dozens of marine sediment cores, we have selected along the continental slope a suite of cores between 28°N and 40°N, including the latitude of Cape Hatteras (Figure 1, Table 1). We relied on the carbonate content, ^{14}C dates, and foraminiferal $\delta^{18}O$ stratigraphies to identify the sediment horizons representing approximately the Last Glacial Maximum and the Holocene, the past 10,000 years characterized by relatively mild climate conditions largely similar to the present.

[8] If the local seawater temperature and to a lesser extent salinity remained unchanged, the Holocene and glacial sediments can be easily identified on the basis of foraminiferal $\delta^{18}O$ stratigraphy alone. During glacial times, more of the lighter oxygen isotope (^{16}O) is locked on land in the form of larger continental ice volume, and the global seawater $\delta^{18}O$ is enriched. The time evolution of seawater $\delta^{18}O$

Table 1. Marine Sediment Cores

Core	Latitude, °N	Longitude, °W	Water Depth, m
	North of 36°30′N		
V15-212	39°00′	72°08′	2173
V4-1	38°53′	70°55′	2867
V21-1	38°43′	72°39′	2186
V26-177	37°33′	72°34′	2979
KZ81-10G	37°42′	73°56′	1616
RC10-289	37°02′	72°31′	3173
	South of 36°30′N		
V21-2	36°05′	70°24′	4455
V26-176	36°03′	72°23′	3942
V30-5	34°37′	74°39′	3203
V26-175	33°56′	74°26′	3995
K140-2 GGC50	32°45′	76°14′	1903
K140-2 JPC22	28°14′	74°24′	4712

is reflected in foraminiferal $\delta^{18}O$ stratigraphy, and glacial sediments are therefore characterized by heavy $\delta^{18}O$ values. The global continental ice volume $\delta^{18}O$ signal over the last deglaciation (i.e., the average seawater $\delta^{18}O$ difference between the Holocene and LGM) is estimated to be between 1.0‰ [*Schrag and DePaolo*, 1993; *Schrag et al.*, 1996] and 1.3‰ [*Fairbanks*, 1989].

[9] Since we are attempting to reconstruct possible changes in the position of the Gulf Stream by detecting for changes in the local seawater temperature (and salinity) that are reflected in foraminiferal $\delta^{18}O$, foraminiferal $\delta^{18}O$ stratigraphy by itself is not appropriate to identify the Holocene and glacial sediments. This is particularly so, because the global ice volume signal is similar to the dynamic range of $\delta^{18}O$ across the Cold Wall, as shown below. That is, if there is ~1‰ change in foraminiferal $\delta^{18}O$ downcore, it would be difficult to determine unequivocally whether the change is due to deglaciation or to a shift in the position of the Gulf Stream.

[10] We therefore use $CaCO_3$ content and radiocarbon data to help identify the Holocene and glacial sediments in most of the cores used in this study. *Balsam* [1981] has shown that the temporal variability of carbonate content in numerous marine sediment cores raised from the western margin of the North Atlantic is highly correlative. In cores from 2500 to 4500 m water depth, carbonate content is typically 20 ~ 30% during the Holocene but is significantly lower during glacial period [*Balsam*, 1981]. The low $CaCO_3$ content in glacial sediments appears to result from a combination of larger influx of terrigenous materials and enhanced dissolution. The transition from low glacial carbonate values to high Holocene values occurs between 14,000 and 8,000 ^{14}C years.

[11] The latitude of Gulf Stream separation is easily identified today by prominent latitudinal changes in temperature and salinity at 250 m water depth (Figure 2), the depth that best reflects the $\delta^{18}O$ signature in *G. truncatulinoides* as discussed below. At this depth, the warm (~19°C) and salty (~36.5‰) Sargasso Seawater is found to the south of about 36°N; to the north of 37°N lies the cold (~10°C) and fresh (~35.2‰) Slope Water. A transition zone between 36°N and 37°N indicates the presence of the Cold Wall. Coincidentally, the 15°C isotherm at 200 m in the central North Atlantic was identified earlier as an indicator for the thermal front associated with the Gulf Stream [*Hansen*, 1970], suggesting that $\delta^{18}O$ of *G. truncatulinoides* is ideally suited to monitor the Gulf Stream. The spatial variability of the 15°C isotherm at 250 m using the Levitus monthly climatology [*Levitus and Boyer*, 1994; *Levitus et al.*, 1994] shows that the seasonal variation in the Gulf Stream position is limited to within 1° latitude near the continent where separation occurs (Figure 1).

[12] Temperature and salinity act in opposite directions on foraminiferal calcite $\delta^{18}O$ (e.g., Sargasso Sea's higher temperatures tend to make the $\delta^{18}O$ lighter but its higher salinities tend to make $\delta^{18}O$ heavier), but the temperature effect predominates for the relevant temperature and salinity ranges. The net effect of the temperature and salinity changes across the Cold Wall at 250 m translate to more than 1.0‰ in foraminiferal calcite $\delta^{18}O$, a dynamic range that is more than an order magnitude larger than the $\delta^{18}O$ measurement precision and thus theoretically easily identified. The select in situ temperature and salinity data at 250 m shown in Figure 2 show no discernable difference between summer and winter. However, an examination of objectively

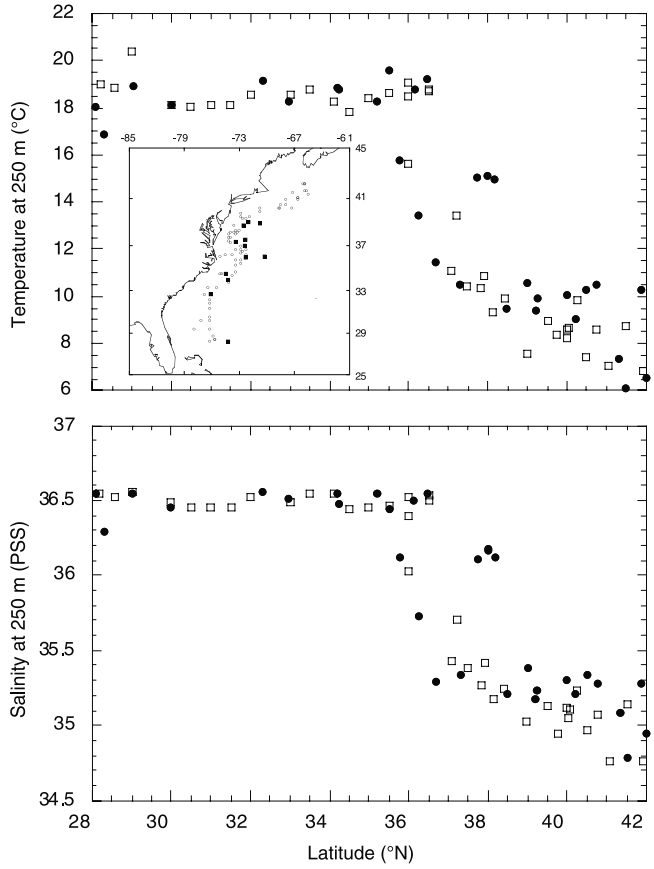

Figure 2. In situ (top) temperature and (bottom) salinity data at 250 m water depth. Solid circles indicate summer (June, July, and August) data, and open squares indicate winter data (December, January, and February). Hydrographic data locations are indicated by open circles and core sites by solid squares (top panel inset). All hydrographic data were obtained online from NOAA (http://www.epic.noaa.gov). The prominent break in temperature and salinity near 36.5°N indicates the boundary between the waters of Sargasso Sea and Slope Water.

Table 2. Radiocarbon Dates[a]

Core	Core Depth, cm	Foraminiferal Species	NOSAMS Accession Number	AMS ^{14}C Age, ^{14}C Years
V30-5	120	Mixed Planktonic	OS-25627	3,180
V30-5	200	Mixed Planktonic	OS-25628	5,570
V30-5	295	Mixed Planktonic	OS-25629	9,220
V30-5	390	Mixed Planktonic	OS-25630	11,600
V30-5	490	Mixed Planktonic	OS-25631	11,500
V30-5	615	Mixed Planktonic	OS-25632	12,000
V30-5	710	Mixed Planktonic	OS-25633	13,650
V30-5	846	Mixed Planktonic	OS-32340	17,650
V21-1	94	Mixed Planktonic	OS-25798	13,300
V21-1	285	Mixed Planktonic	OS-25799	11,850
V21-1	411	Mixed Planktonic	OS-32338	19,450
V21-1	922	Mixed Planktonic	OS-32339	26,300
RC10-289	105	Uvigerina spp.	OS-25801	16,650
RC10-289	180	Uvigerina spp.	OS-25800	16,750
KZ81-10G	152	Mixed Planktonic	OS-25802	7,410
KZ81-10G	190	Mixed Planktonic	OS-26051	8,320

[a]Reservoir age correction of 400 ^{14}C years is applied to AMS ^{14}C age measured on planktonic foraminifera [*Bard*, 1988]. A correction of 1000 ^{14}C years is applied to benthic foraminifera that accounts for the 400 ^{14}C years of the surface reservoir age and an apparent ventilation age of the glacial deep Atlantic of about 600 ^{14}C years [*Broecker et al.*, 1990].

analyzed hydrographic data [*Levitus and Boyer*, 1994; *Levitus et al.*, 1994] at 250 m in the western North Atlantic indicates seasonal temperature and salinity variabilities of respectively 0.6°C and 0.15‰. These variabilities give a combined uncertainty of ±0.1‰ in calcite δ^{18}O.

[13] We made δ^{18}O measurements on multiple, encrusted individuals of deep-dwelling planktonic foraminifera *Globorotalia truncatulinoides* (>425 μm) to identify this 1.0 ± 0.1‰ latitudinal δ^{18}O gradient. While the calcification process of this species is not simple, *Mulitza et al.* [1997] show that the δ^{18}O of encrusted *G. truncatulinoides* reflects temperatures at 250 m water depth in the equatorial and South Atlantic. This is somewhat surprising, given that *G. truncatulinoides* initially calcify in surface waters in the subtropics [*Hemleben et al.*, 1985; *Deuser and Ross*, 1989; *Lohmann and Schweitzer*, 1990] and add up to 50% of shell mass during its descent down to ~700 m [*Lohmann and Schweitzer*, 1990]. The surprising correlation of the δ^{18}O of the shell and the subsurface temperature at 250 m appears to result from the correlation of 250 m temperature and water column stratification [*Mulitza et al.*, 1997]. Although *G. truncatulinoides* begin to calcify in surface waters in the subtropics, they tend to do so in early spring when deep vertical mixing by winds weaken stratification [*Hemleben et al.*, 1985]. The δ^{18}O of shell in this case would not be very different from δ^{18}O of shell calcified deeper (i.e., 250 m), because the water column stratification is weak. In the tropics, where stratification is strong, *G. truncatulinoides* calcification starts below the pycnocline in waters with temperatures close to the 250 m temperature. So while the actual calcification of *G. truncatulinoides* appears to be complex, the δ^{18}O signature of *G. truncatulinoides* is primarily acquired below the surface, and, in today's ocean, reflects water column properties at a depth of approximately 250 m.

[14] In addition to *G. truncatulinoides*, a limited number of δ^{18}O was measured on near-surface dwelling planktonic foraminifera *Globigerinoides sacculifer* and *Globigerinoides ruber*. All three species prefer warm waters, and are abundant in sediments underlying the Gulf Stream but rare in sediments underlying the Slope Water. This is especially so in glacial sediments, whose carbonate content is very low. Consequently, glacial δ^{18}O measurements are much fewer.

[15] To estimate the equilibrium calcite δ^{18}O as a function of ambient seawater δ^{18}O and temperature, we use the equation for *Cibicidoides* species [*Lynch-Stieglitz et al.*, 1999a], which is nearly the same as that for inorganically precipitated calcite [*Kim and O'Neil*, 1997] and cultured planktonic foraminifera [*Bemis et al.*, 1998]. As for seawater δ^{18}O, we use the salinity-δ^{18}O relationship from *Lynch-Stieglitz et al.* [1999a], who used the western North Atlantic data (T > 5°C) of the Geochemical Ocean Sections Survey. A salinity-δ^{18}O relationship for the Slope Water [*Fairbanks et al.*, 1992] is sufficiently similar that there is no significant difference in the final estimate of calcite δ^{18}O using either formulae.

[16] All stable isotope ratio measurements were made at Lamont-Doherty Earth Observatory on a Micromass Optima fitted with a Multiprep carbonate preparation device. The machine is calibrated with NBS-18 and NBS-19 and all values are reported versus VPDB. Repeat analyses of in-house standards larger than 30μg (n = 78) indicate a precision of ±0.08‰ for δ^{18}O and ±0.05% for stable carbon isotope composition (δ^{13}C). The overall precision (n = 102) including smaller samples is ±0.09‰ for δ^{18}O and ±0.06% for δ^{13}C. Weight percent $CaCO_3$ was analyzed at Lamont-Doherty Earth Observatory using standard coulometric titrimetry following acidification with hydrochloric acid, with a precision of ±1%. All new radiocarbon dates were obtained on foraminiferal shell samples at the National Ocean Sciences AMS Facility at the Woods Hole Oceanographic Institution.

3. Results

[17] All new radiocarbon dates are summarized in Table 2. All new isotope data as well as the number of *G. truncatulinoides* shells used for each measurement are presented in Table 3. Carbonate content is presented in Figure 3 along with new and previous ^{14}C dates. Data from cores south of today's Gulf Stream separation (36.5°N) are plotted against

Table 3. New Planktonic Foraminiferal $\delta^{18}O$ Data[a]

	G. truncatulinoides			*G. saculifer*		*G. ruber*		
Core Depth, cm	$\delta^{13}C$, ‰	$\delta^{18}O$, ‰	Number	$\delta^{13}C$, ‰	$\delta^{18}O$, ‰	$\delta^{13}C$, ‰	$\delta^{18}O$, ‰	Time Slice
				K140-2 JPC22 (28.3°N)				
3	1.39	0.43	5	2.48	−1.25	2.21	−1.49	H
5	1.34	0.41	5	2.32	−1.27	1.79	−1.63	H
161	1.18	1.73	5			0.62	0.47	G
179	1.29	1.78	3					G
				K140-2 GGC50 (32.8°N)				
5	1.32	0.49	8	2.69	−1.38	1.94	−1.78	H
9	1.23	0.39	7	2.08	−1.33	1.94	−1.67	H
253	1.23	1.30	3	1.90	0.29	1.65	−0.30	G
				V26-175 (33.9°N)				
5	1.10	0.56	10					H
15	1.14	0.61	10					H
25	1.00	0.94	10					H
35	1.18	0.39	8					H
53	1.22	0.56	3					
63	1.26	0.44	3					
71	0.91	1.25	8					
75	1.00	1.66	10					
81	0.94	1.23	8					
85	0.86	1.24	10					
90	0.85	1.18	6					
115	1.21	1.34	10					
135	1.16	1.32	3					G
155	1.22	1.39	6					G
165	1.09	1.40	5					G
175	0.99	1.44	8					G
				V30-5 (34.6°N)				
15	1.46	0.73	5	2.48	−1.05	1.72	−1.69	H
25	1.20	0.73	5	2.12	−1.40	2.52	−1.88	H
35	1.30	0.50	7	1.97	−1.64	1.89	−1.92	H
45	1.33	0.42	7	2.24	−1.54	2.15	−1.90	H
55	1.21	0.50	6	2.47	−1.25	1.71	−2.07	H
65	1.16	0.40	7	2.26	−1.39	1.96	−1.82	H
75	1.08	0.35	7	2.66	−1.84	1.73	−2.05	H
85	1.27	0.36	8	2.37	−1.72	1.92	−1.89	H
95	1.21	0.38	8	2.19	−1.55	1.58	−1.84	H
105	1.20	0.34	8	2.67	−1.56	1.63	−1.82	H
115	1.07	0.44	7	2.16	−1.69	1.50	−1.88	H
125	0.98	0.38	7	2.44	−1.61	1.88	−1.88	H
135	1.19	0.34	7	2.05	−1.62			H
145	1.18	0.29	7	2.10	−1.80			H
155	1.11	0.30	7	2.19	−1.69	1.94	−2.14	H
165	1.11	0.35	7	2.23	−1.52	1.99	−2.19	H
175	1.30	0.39	7	2.04	−1.51	2.05	−2.03	H
185	1.21	0.68	7					H
195	1.16	0.59	6					H
205	1.17	0.64	6					H
215	1.18	0.51	6					H
225	1.05	0.51	6					H
235	1.10	0.49	5					H
255	1.06	0.63	5					H
265	0.90	0.66	10					H
281	0.83	0.38	10	2.15	−1.09			H
295	0.90	0.61	6					H
309	0.85	0.43	7	1.70	−0.74			H
315	0.68	1.29	6	1.27	−0.37			
335	0.88	1.21	6					
351	1.12	1.54	5					
365	0.84	1.09	9	1.68	−0.44			
375	0.70	1.17	6					
385	0.77	0.95	10	1.97	−0.48			
400	0.87	1.07	7	2.06	−0.58			
415	0.76	1.02	6					
422	0.72	0.84	10	2.26	−0.70			
435	0.77	1.36	3	1.89	−0.37			
455	0.90	1.59	6					
468	0.88	1.27	6					
485	0.82	1.19	10					

Table 3. (continued)

	G. truncatulinoides			*G. saculifer*		*G. ruber*		
Core Depth, cm	$\delta^{13}C$, ‰	$\delta^{18}O$, ‰	Number	$\delta^{13}C$, ‰	$\delta^{18}O$, ‰	$\delta^{13}C$, ‰	$\delta^{18}O$, ‰	Time Slice
495	0.78	1.41	6					
505	0.89	0.91	6					
518	0.77	0.97	6	1.13	0.40			
525	0.55	0.91	4					
535	0.91	1.08	6					
545	0.88	1.13	5					
565	0.82	1.02	3					
575	0.98	1.53	4					G
585	0.94	1.66	2					G
596	1.03	1.58	6					G
615	1.03	1.65	6					G
634	0.89	1.53	2					G
656	1.09	1.77	6					G
669				1.50	−0.65			G
685	1.09	1.56	10	1.45	−0.14			G
705	1.02	1.66	6					G
720	1.11	1.53	6					G
731	1.52	17.30				1.11	0.31	G
743	1.00	1.41	3	1.48	0.92	1.47	−0.29	G
751	0.98	1.12				1.10	−0.09	G
761	1.27	1.92	3	1.58	0.51	1.10	0.05	G
768	1.18	1.57	3	0.90	−1.15	0.97	0.06	G
781	1.26	1.94	3	1.77	0.61	0.92	−0.28	G
791	1.00	1.69	3			1.07	−0.15	G
801	1.28	1.74	2	1.41	0.21	1.17	−0.22	G
811	1.28	1.53	3	1.27	0.38	1.08	−0.19	G
821	0.90	1.26	3	1.50	0.30	1.16	−0.09	G
831						1.28	−0.19	G
841	1.19	1.95	3	1.23	0.31	1.16	0.13	G
847	1.30	1.79	2	1.45	0.38	1.28	0.19	G
				V26-176 (*36.0°N*)				
15	1.08	0.36	4	1.76	−1.12			H
24	1.08	0.38	3	2.61	−1.22			H
35	1.17	0.35	6	2.56	−1.04			H
57	1.31	0.49	6	2.01	−1.50			H
68	1.14	0.29	8	2.15	−0.90			H
88	1.05	0.34	7	2.51	−1.42			H
254	0.90	1.05	2	1.59	−0.63			G
264	0.99	1.61	3	1.93	−0.68			G
275	1.06	1.38	2	1.27	−0.98			G
295	0.70	1.37	3	1.65	−0.34			G
317				1.63	−0.05			G
				V21-2 (*36.1°N*)				
5	1.14	0.64	6					H
46	1.12	0.41	6					H
75	0.99	0.55	6					H
125	0.93	0.73	6					H
165	0.92	0.90	6					H
195	0.55	0.75	6					H
				RC10-289 (*37.0°N*)				
15	1.24	0.98	10	2.63	−1.46			H
25	1.27	0.91	2	2.35	−1.33	1.91	−1.83	H
35	1.20	0.66	10	2.11	−1.20	1.90	−1.58	H
45	1.32	1.40	10	2.22	−1.09	1.82	−1.83	
55	1.31	1.21	10	2.69	−1.36	2.04	−1.36	
65				2.34	−1.45	2.27	−2.19	
65	1.33	0.88	2					
75				2.36	−1.36	2.17	−1.44	
88						0.51	0.65	
92	1.00	2.16	2					
95						1.19	0.10	
115						0.63	−0.10	
116	0.90	1.49	3					
125				1.09	1.32	0.59	−0.52	
135	1.11	2.61	3			1.71	−0.78	G
145						0.80	0.44	G
155	1.14	1.90	2					G
165	1.05	1.76	4			0.83	−0.11	G

Table 3. (continued)

	G. truncatulinoides			*G. saculifer*		*G. ruber*		
Core Depth, cm	$\delta^{13}C$, ‰	$\delta^{18}O$, ‰	Number	$\delta^{13}C$, ‰	$\delta^{18}O$, ‰	$\delta^{13}C$, ‰	$\delta^{18}O$, ‰	Time Slice
175	0.69	1.82	2					G
				KZ81-10G (37.4°N)				
33	1.25	1.50	4					H
45	1.11	1.30	2					H
54	1.35	1.60	2					H
96	1.25	1.74	4					H
152	0.60	1.22	3					H
				V26-177 (37.6°N)				
25				2.20	−2.16			H
35	1.31	1.64	4	2.07	−1.84			H
45	1.23	1.16	2	2.14	−1.97			H
55				2.11	−1.90			H
65	1.40	1.40	5	2.09	−1.73			H
75				2.07	−1.59			H
85				1.79	−1.96			H
105	1.01	1.60	2	1.82	−1.78			H
115				1.39	−1.44			H
125	0.60	0.71	2	1.94	−1.41			H
135	1.01	1.29	5	1.28	−1.41			H
155				1.75	−1.51			H
165				1.29	0.08			H
175				1.36	−2.12			H
				V21-1 (38.7°N)				
15	1.08	1.60	10	2.50	−1.01	1.91	−1.97	H
35	1.08	1.61	10	2.59	−0.70	1.70	−1.89	H
75	1.29	1.50	10	2.13	−0.94	2.03	−1.69	H
248	0.95	2.86	2					G
268	0.16	2.15	2					G
300	0.75	2.63	2					G
				V4-1 (38.9°N)				
0 (TW)	1.32	1.72	5	2.09	−0.80	1.90	−1.89	H
30	1.48	1.88	4	2.32	−0.65			H
90				2.03	−1.21			H
100				1.82	−1.42			H
120						1.39	−1.61	H
198	1.20	1.88	8					
200	0.94	2.35	6					
288	0.55	2.45	3					G
582	1.09	2.15	5					G
629	1.31	2.57	2					G
				V15-212 (39.0°N)				
15	1.28	1.56	5					H

[a]In the Time Slice column, H = Holocene and G = glacial as determined from a combination of carbonate stratigraphy, radiocarbon dates, and $\delta^{18}O$ stratigraphy. TW = trigger weight core.

core depth in Figure 4. Likewise, downcore data from north of 36.5°N are presented in Figure 5. The Holocene and glacial $\delta^{18}O$ values are identified in Table 3 (last column) and summarized in Table 4. Finally, the time slice latitudinal $\delta^{18}O$ profiles are shown in Figures 6 and 7.

3.1. Downcore $CaCO_3$ Content and $\delta^{18}O$ Data

[18] Many of the cores used in this study were previously examined by *Balsam* [1981] for carbonate content. We made additional carbonate content measurements and confirm that the general pattern of low glacial%$CaCO_3$ and high Holocene%$CaCO_3$ hold for most cores, with the exception of KZ81-10G (Figure 3). Throughout this core, the carbonate content does not vary much and is about half the typical Holocene carbonate content seen in cores from 2500 $\sim$ 4500 m. The KZ81-10G radiocarbon dates corrected for reservoir-age at 152 and 190 cm are both less than 8,000 ^{14}C years (Figure 3), placing the dates clearly in the Holocene. The relatively low carbonate content of this core is likely a result of dilution by a large terrigenous material influx because of its shallow water depth at 1616 m. Another core that does not display the glacial-interglacial change in%$CaCO_3$ is V21-2, whose elevated carbonate content and radiocarbon dates younger than 10,000 ^{14}C years clearly indicate that core bottom at 200 cm has not reached glacial sediments (Figure 3).

[19] We did not measure carbonate content on K140-2 JPC22 and K140-2 GGC50, whose glacial and Holocene samples and detailed *G. ruber* $\delta^{18}O$ stratigraphies (Figure 4) were provided by L. Keigwin of Woods Hole Oceanographic Institution. These $\delta^{18}O$ stratigraphies can be interpreted largely in terms ice volume changes and thus serve as

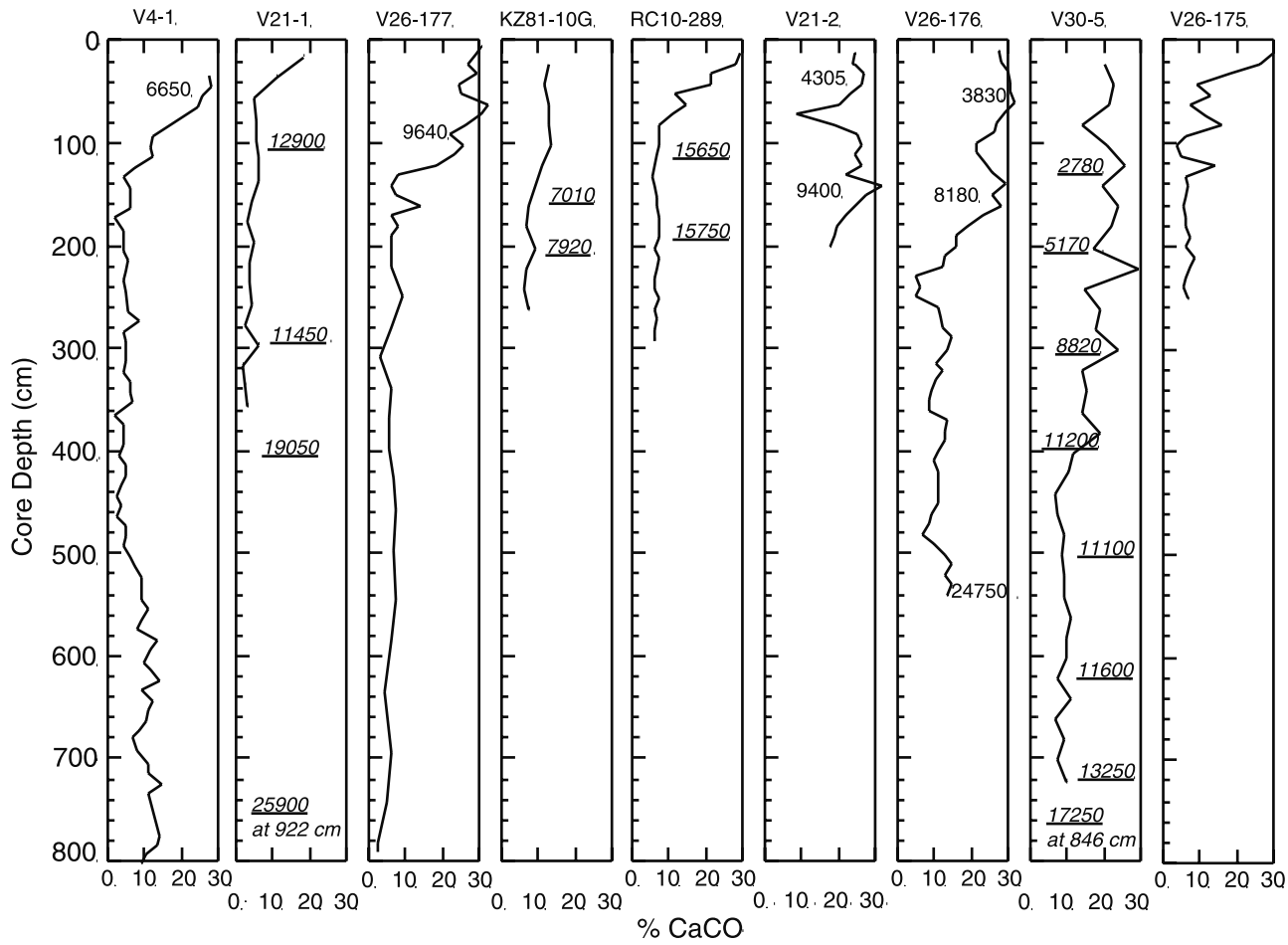

Figure 3. Downcore $CaCO_3$ content and radiocarbon. Carbonate data from V4-1, V26-177, RC10-289, V21-2, V26-176, and V26-175 are from *Balsam* [1981] as are ^{14}C dates from V4-1, V26-177, V26-176. Radiocarbon dates from V21-2 are from *Ledbetter and Balsam* [1985]. The reservoir-age corrected new AMS ^{14}C dates (Table 2) are underlined and italicized.

chronology. Because these cores are farthest from the Gulf Stream separation latitude, their $\delta^{18}O$ stratigraphies are not likely to be affected by changes in separation latitude.

[20] Carbonate content was also not measured on V15-212, from which only one $\delta^{18}O$ measurement could be obtained (Figure 5). We assumed the single datum to represent the Holocene, because it was obtained at 15 cm from the core top and its $\delta^{18}O$ value is regionally consistent with Holocene $\delta^{18}O$ values from other cores as shown below.

[21] The two shallowest radiocarbon dates from V21-1 suggests an age reversal, since the topmost date at 94 cm is 12,900 ^{14}C years and the next date at 285 cm is somewhat younger at 11450 ^{14}C years (Figure 3). If real, this would indicate some sediment disturbance, apparently involving pre-Holocene sediments. The data from this core therefore need to be viewed with some caution. The third and fourth dates from this core further down are progressively larger in ^{14}C age and do not show signs of reversal. There is also a 100-year reversal in V30-5 dates at 390 and 490 cm, but this reversal is within the analytical error.

[22] The foraminiferal $\delta^{18}O$ stratigraphies from cores south of the Gulf Stream separation today (Figure 4) and from the north (Figure 5) are consistent with the chronology offered by carbonate content: $\delta^{18}O$ is lighter in Holocene sediments indicated by high $CaCO_3$% and $\delta^{18}O$ is heavier in glacial sediments indicated by low carbonate content. Because of the lack of foraminiferal tests, glacial $\delta^{18}O$ measurements could not be obtained from V21-2, V26-177, and V15-212, as well as from KZ81-10G. For the same reason, we could not obtain more than the sixteen new radiocarbon dates (Table 2).

[23] We are able to quite clearly separate the Holocene and glacial sediments from a combination of carbonate content stratigraphy, radiocarbon dates, and foraminiferal $\delta^{18}O$ stratigraphy. However, it is difficult to say whether the glacial sediments that we have identified represent the LGM, about a 3000-year window in time, and this is perhaps the largest source of uncertainty in this study. Therefore the data that we call "glacial" should be interpreted to refer to a slightly broader time window, representing the late last glacial cycle.

3.2. Time Slice Latitudinal $\delta^{18}O$ Profiles

[24] The Holocene *G. truncatulinoides* $\delta^{18}O$ measurements plotted versus latitude clearly show a prominent

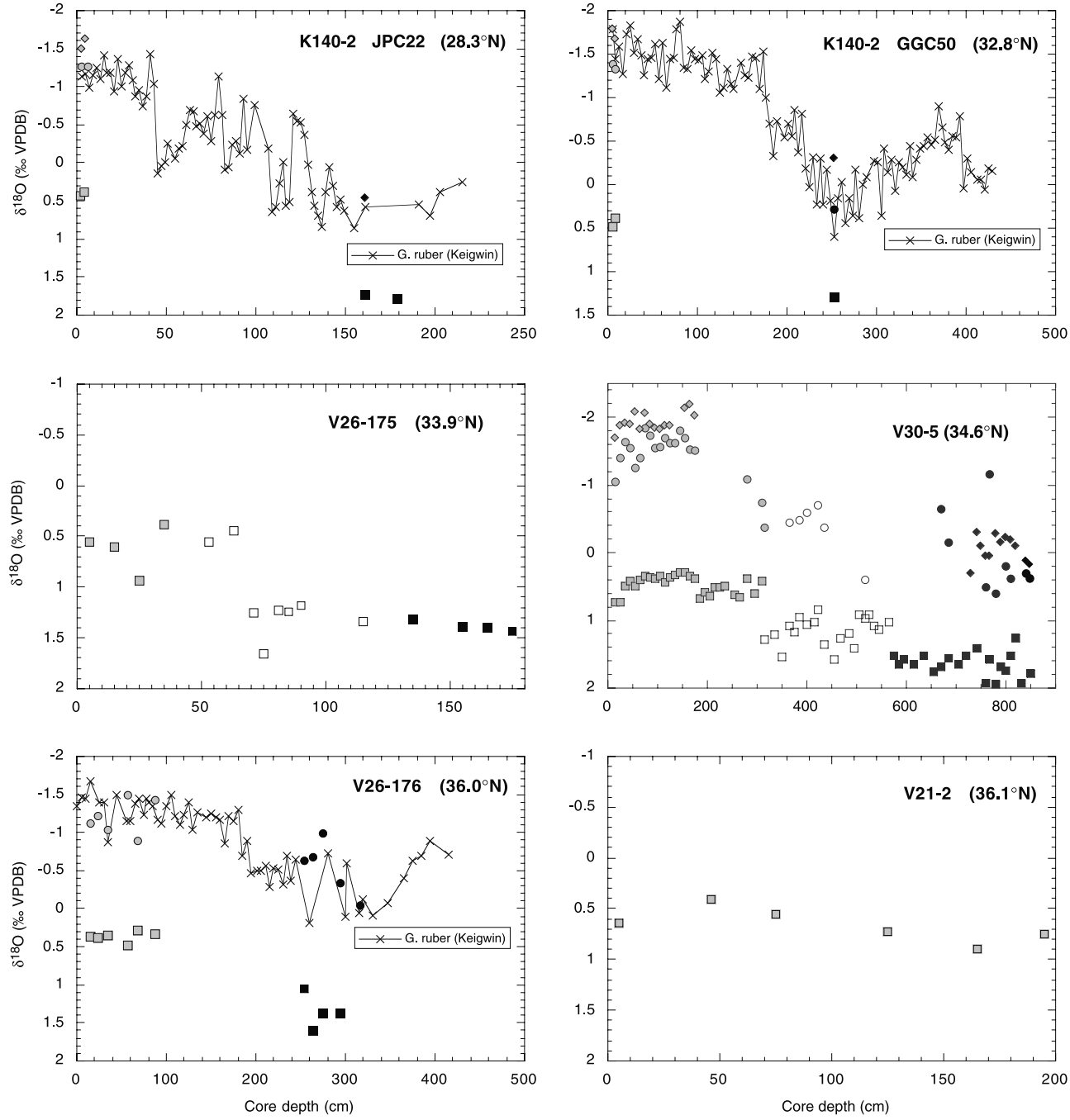

Figure 4. New downcore $\delta^{18}O$ data from cores in the Sargasso Sea regime, from south of 36.5°N: *G. truncatulinoides* (squares), *G. sacculifer* (circles), and *G. ruber* (diamonds). *G. ruber* $\delta^{18}O$ data from the two K140-2 cores were provided by L. Keigwin (unpublished data, 2000), and those from V26-176 are from *Keigwin and Jones* [1989]. See Table 3 for individual data. Shaded symbols indicate Holocene time slice values, and solid symbols indicate glacial values, summarized in Table 4.

break near the latitude of modern Gulf Stream separation (Figure 6). The *G. truncatulinoides* $\delta^{18}O$ reflecting the subtropical waters are approximately 0.5‰ to the south of 36°N. To the north of 37°N, the Slope Water *G. truncatulinoides* $\delta^{18}O$ are about 1.5‰. The water mass boundary and hence the Gulf Stream separation as seen by *G. truncatulinoides* occurs within approximately 1° in latitude. This sharp *G. truncatulinoides* $\delta^{18}O$ gradient agrees well with the estimated calcite $\delta^{18}O$ formed under equilibrium with seawater temperatures and salinities at 250 m (Figure 6). The agreement confirms our hypothesis that the Gulf Stream position can be identified with a latitudinal distribution of *G. truncatulinoides* $\delta^{18}O$. However, the agreement in terms of absolute $\delta^{18}O$ values is surprising, given what we know about the complexity of the ecology of *G. truncatulinoides* and the uncertainty involved in characterizing the average Holocene $\delta^{18}O$ values from a limited number of measurements (Table 4).

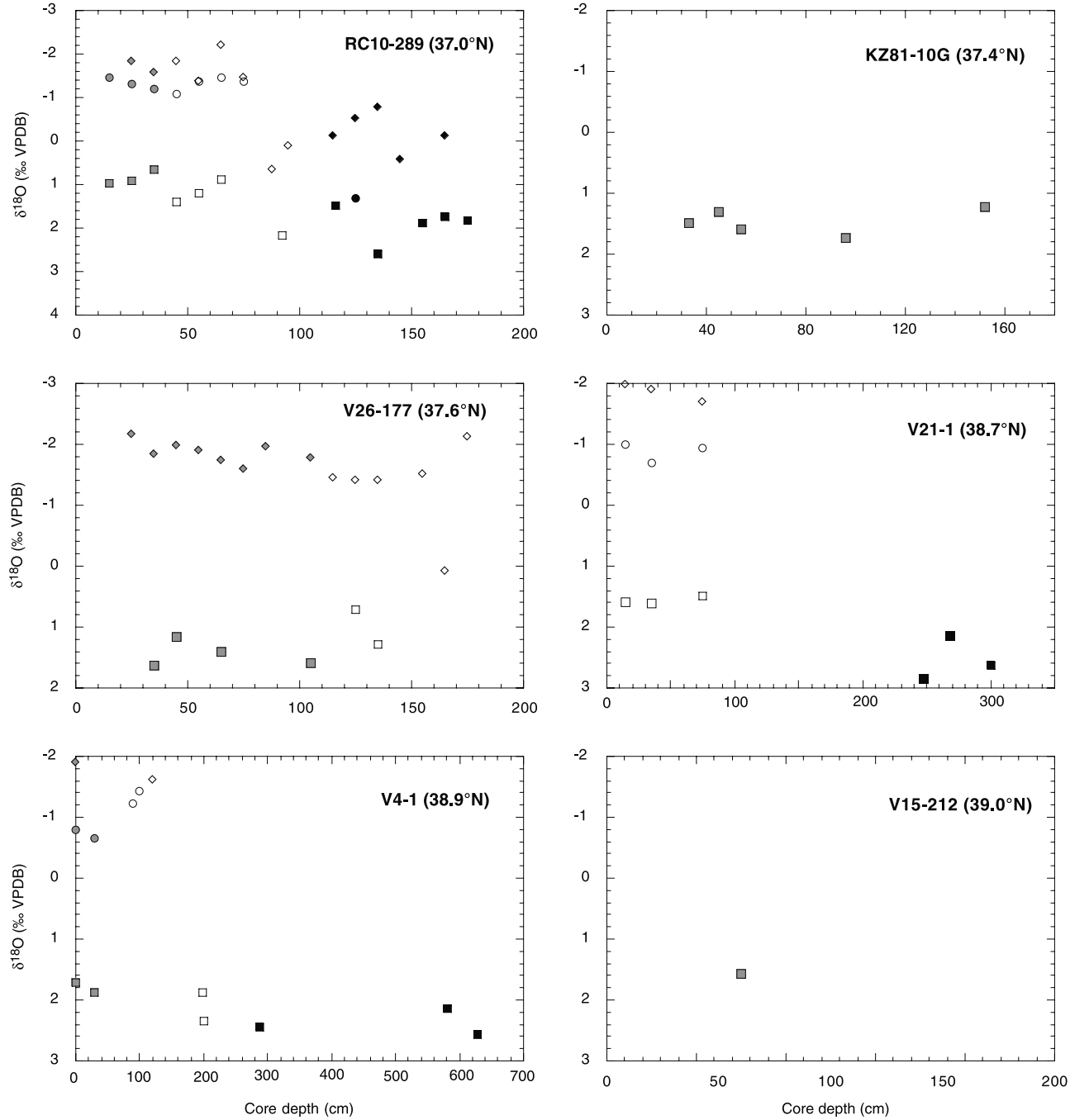

Figure 5. New downcore $\delta^{18}O$ data from cores in the Slope Water regime, north of 36.5°N. See Figure 4 caption for legend.

The agreement and constancy of the Holocene $\delta^{18}O$ suggest that the Gulf Stream separation near Cape Hatteras remained a robust oceanographic feature during much of the Holocene.

[25] The Holocene $\delta^{18}O$ of surface dwelling *G. sacculifer* and *G. ruber* in contrast do not reflect the Cold Wall (Figure 6). *G. sacculifer* $\delta^{18}O$ remains nearly constant at 1.2‰ across the latitude of Gulf Stream separation; likewise, *G. ruber* $\delta^{18}O$ is nearly uniform at 1.7‰. An examination of surface water hydrography indicates that these surface dwelling foraminifera calcify during the summer (Figure 6). An analysis of sediment trap samples at 125 m water depth anchored on the continental slope of the Middle Atlantic Bight (~38°N) confirms that *G. ruber* production peaks in the summer [*Brunner and Biscaye*, 1997]. Summer insolation warms even the Slope Water to temperatures in excess of 20°C at the surface, thereby largely muting the gradients across the Cold Wall of surface temperatures and $\delta^{18}O$ of foraminifera calcifying in these waters. Although not presented here, the winter surface waters in contrast shows prominent thermal and salinity gradients across the Cold Wall with absolute values of temperature and salinity nearly indistinguishable from those at 250 m (Figure 2) due apparently to deep winter mixing.

Table 4. Holocene and Glacial Planktonic Foraminiferal $\delta^{18}O$ Data[a]

	G. truncatulinoides				*G. sacculifer*				*G. ruber*			
	Holocene		LGM		Holocene		LGM		Holocene		LGM	
Core	n	$\delta^{18}O$	n	$\delta^{18}O$	n	$\delta^{18}O$	n	$\delta^{18}O$	n	$\delta^{18}O$	n	$\delta^{18}O$
						North of 36°30'						
V15-212	1	1.56										
V4-1	2	1.80 ± 0.08	3	2.39 ± 0.18	4	−1.02 ± 0.36			2	−1.75 ± 0.20		
V21-1	2	1.60 ± 0.01	3	2.54 ± 0.30	3	−0.88 ± 0.16			3	−1.85 ± 0.15		
V26-177	4	1.45 ± 0.19							12	−1.73 ± 0.25		
KZ81-10G	5	1.47 ± 0.19										
RC10-289	3	0.85 ± 0.14	5	1.96 ± 0.37	7	−1.32 ± 0.13	1	1.31	6	−1.71 ± 0.31	7	−0.05 ± 0.50
						South of 36°30'						
V21-2	6	0.66 ± 0.17										
V26-176	6	0.37 ± 0.07	4	1.35 ± 0.20	6	−1.20 ± 0.23	5	−0.53 ± 0.36				
V30-5	28	0.47 ± 0.13	20	1.65 ± 0.17	17	−1.48 ± 0.24	8	0.05 ± 0.59	15	−1.93 ± 0.14	13	−0.06 ± 0.19
V26-175	4	0.63 ± 0.20	4	1.39 ± 0.04								
K140-2 GGC50	2	0.44 ± 0.07	1	1.30	2	−1.36 ± 0.04	1	0.29	2	−1.73 ± 0.08	1	−0.30
K140-2 JPC22	2	0.42 ± 0.01	2	1.76 ± 0.03	2	−1.26 ± 0.01			2	−1.56 ± 0.10	1	0.47

[a]All $\delta^{18}O$ data are reported in the units of per mil (‰) versus VPDB. See Table 3 for data used to obtain these averages.

[26] The glacial latitudinal *G. truncatulinoides* $\delta^{18}O$ profile is strikingly similar to the Holocene profile and shows a prominent gradient of ~1.0‰ near 36.5°N (Figure 7). The glacial *G. truncatulinoides* $\delta^{18}O$ trend is captured well by the estimated calcite $\delta^{18}O$ in equilibrium with modern seawater, accounting for the global continental ice volume change. Therefore the Cold Wall and hence the Gulf Stream separation as recorded by *G. truncatulinoides* appear to be located at the same latitude during the Holocene and the last glacial. The relatively large standard deviations of the glacial $\delta^{18}O$ and their lower spatial resolution however prevent the determination of the glacial separation latitude within one degree. The mean glacial separation latitude seems securely bounded within two degrees by the clearly subtropical $\delta^{18}O$ of 1.35 ± 0.20‰ at 36.0°N (V26-176) and subpolar $\delta^{18}O$ of 2.54 ± 0.30‰ at 38.7°N (V21-1) (Figure 7, Table 4). Located between the two $\delta^{18}O$ data is an intermediate value of 1.96 ± 0.37‰ at 37.0°N (RC10-289), whose large ±0.37‰ uncertainty makes it difficult to elucidate the exact structure of the $\delta^{18}O$ gradient. The Gulf

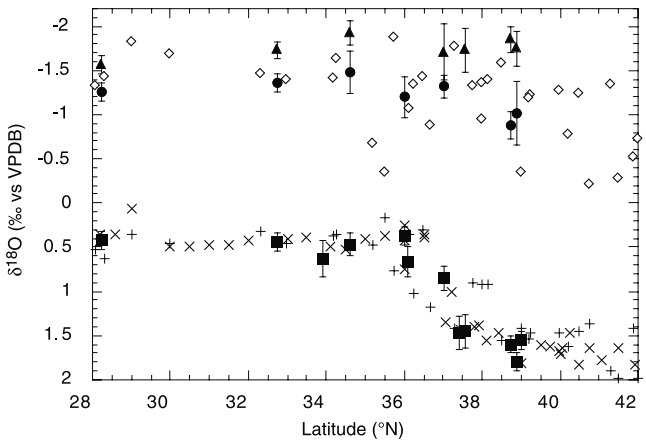

Figure 6. Holocene $\delta^{18}O$ of *G. truncatulinoides* (solid squares), *G. sacculifer* (solid circles), and *G. ruber* (solid triangles) versus latitude. The error bars for *G. truncatulinoides* $\delta^{18}O$ represent 0.2‰ calcite $\delta^{18}O$ variability expected from seasonal variability in temperature and salinity at 250 m or standard deviations of time slice averages, whichever is larger. Shown in cross (winter) and plus (summer) symbols are estimated calcite $\delta^{18}O$ in equilibrium with temperatures and salinities at 250 m presented in Figure 2. Equilibrium calcite $\delta^{18}O$ for summer surface waters are shown in open diamonds. Note that $\delta^{18}O$ of deep-dwelling *G. truncatulinoides* captures the sharp hydrographic boundary at 36°N ~ 37°N between the warm and salty Sargasso Sea and cold and fresh Slope Water.

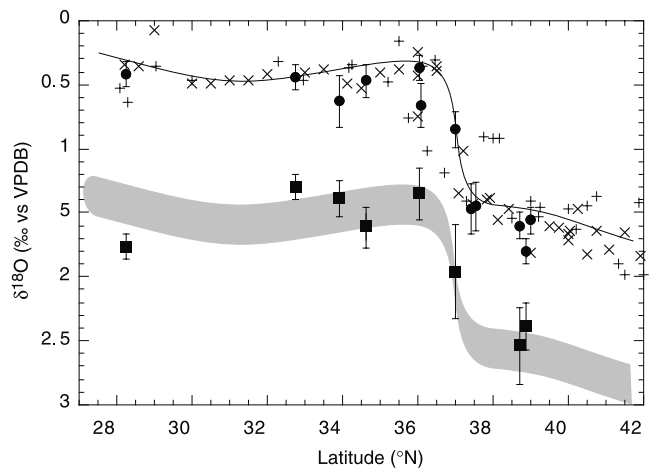

Figure 7. Last Glacial Maximum (solid squares) $\delta^{18}O$ of *G. truncatulinoides* versus latitude. Replotted from Figure 6 are Holocene *G. truncatulinoides* $\delta^{18}O$ (solid circles) and estimated calcite $\delta^{18}O$ in equilibrium with modern ambient seawater (cross and plus symbols are respectively winter and summer). The solid line is an "eye-ball" fit to the equilibrium calcite $\delta^{18}O$. Shaded band shows the expected range of equilibrium calcite $\delta^{18}O$ during the last glaciation, assuming no significant change in the position of the Gulf Stream separation. It is obtained by shifting the solid line 1.0% [*Schrag and DePaolo*, 1993; *Schrag et al.*, 1996] and 1.3‰ [*Fairbanks*, 1989] toward heavier values to account for the larger global continental ice volume.

Stream separation latitude during the Holocene and the last glacial was similarly located, with the glacial latitude of separation within one degree of that for the Holocene.

4. Implications for the Gulf Stream Separation Theories

[27] One of the older theories calls on the winds to induce Gulf Stream separation from the western margin. The close geographical coincidence of the time-mean position of vanishing wind stress curl [*Isemer and Hasse*, 1987] and the Gulf Stream axis after separation lends support for a wind-forced separation. The line of vanishing curl is largely parallel to the Gulf Stream axis but shifted 1° $\sim$ 2° to the south. There also appears to be statistically significant correlation between 2-year lagged Gulf Stream positions, mostly after separation, and the North Atlantic Oscillation [*Taylor and Stephens*, 1998] and El Niño-Southern Oscillation events [*Taylor et al.*, 1998]. The correlation suggests that the Gulf Stream position may be sensitive to changes in surface wind fields. Theoretical basis for the wind-forced separation originates from the early work on the dynamics of wind-driven gyres [*Stommel*, 1948; *Munk*, 1950]. In the simple case of a homogeneous medium in a rectangular flat-bottom basin forced by a meridionally symmetric wind stress τ, the $\nabla \times \tau = 0$ line delimits the boundary between large-scale gyres. A meridional transport across the line is not permitted and the purely zonal flow is fed by the western boundary. This behavior indicates that the $\nabla \times \tau = 0$ line has a causal relationship with the mean axis of the separated Gulf Stream and may even determine the point of separation.

[28] At the time of LGM the Laurentide Ice Sheet over the North American continent reached its maximum size. Simulations of glacial atmospheric circulation consistently indicate that winds in general were stronger due to a steeper meridional surface temperature gradient and that the jet stream, which today is strongest near 60°N, was split by the imposing Laurentide Ice Sheet. Early simulations of atmospheric circulation using the LGM boundary conditions of *CLIMAP Project Members* [1981] indicate that the stronger southern limb of the split jet stream and the surface westerlies, which mimic the high altitude jet stream, were located at around 40°N $\sim$ 45°N [*Gates*, 1976; *Kutzbach and Guetter*, 1986]. More recent simulations using a revised reconstruction of Laurentide Ice Sheet of *Peltier* [1994], which is about half the size of CLIMAP ice sheet, show that the glacial jet stream is still split but less prominently so [*Ramstein and Joussaume*, 1995; *Pollard and Thompson*, 1997; *Bartlein et al.*, 1998; *Kutzbach et al.*, 1998; *Bush and Philander*, 1999; *Broccoli*, 2000]. As in earlier simulations, the surface westerlies are still displaced southward in these recent simulations but only by perhaps a few degrees latitude. Nevertheless, according to the wind-forced separation theory, these glacial winds should cause the Gulf Stream to separate at a more southerly latitude compared to the modern, a prediction that is inconsistent with our reconstruction.

[29] As noted above, the theoretical relationship between the $\nabla \times \tau = 0$ line and the mean axis of the Gulf Stream arises under highly idealized case, where a homogeneous medium in a rectangular flat-bottom basin is forced by meridionally symmetric wind stress. However, the special role of the $\nabla \times \tau = 0$ line breaks down under a more realistic, meridionally asymmetric forcing [*Rhines and Schopp*, 1991]. When the large-scale pattern of wind field is tilted from southwest to northeast, the zonal component of the Sverdrup flow can cross the tilted $\nabla \times \tau = 0$ line, while the meridional component is still prohibited by Sverdrup dynamics from crossing the line. In this case, the line of zero wind stress curl and the gyre boundary no longer coincide especially in the western boundary. For this reason, *Dengg et al.* [1996] conclude that the wind field is probably not the primary cause of separation, although they do not dismiss the idea entirely given the close spatial correspondence in the observed mean position of the Gulf Stream axis and the line of $\nabla \times \tau = 0$. That the Gulf Stream separation remained unchanged during LGM despite a probable southerly shift in the maximum westerlies by a few degrees suggests that the observed spatial correspondence is more of a coincidence.

[30] What then could have pegged the Gulf Stream separation at the latitude of Cape Hatteras during the glacial time? Obvious choices have to do with the geometry of the ocean basin around Cape Hatteras, which remain unchanged over glacial-interglacial timescale. The LGM sea ice edge apparently expanded to ~45°N [*CLIMAP Project Members*, 1981], which is still far too north to pose as a virtual coast for the glacial Gulf Stream.

[31] One aspect of the ocean basin geometry around Cape Hatteras that is rather unique is the curvature of the continental slope. The Gulf Stream may be forced to separate from the coast due to inertial overshooting, if the curvature is simply too sharp for the current to adjust given its large volume transport and inertia [*Dengg et al.*, 1996]. If the Gulf Stream inertia during the glacial time were larger or at least comparable to today, then this theory would predict the separation to occur at Cape Hatteras and be consistent with our reconstruction. If Gulf Stream has more than enough inertia to overshoot today, the current is also expected to overshoot even for a reduced flow, so long as the reduction is less than the ''extra'' inertia. Whether the modern Gulf Stream has an extra inertia however is not known, but there is an indication that the glacial Gulf Stream was perhaps weaker than today. A reconstruction of the Gulf Stream volume transport through the Florida Straits shows that the LGM baroclinic transport was reduced to two thirds of the modern value [*Lynch-Stieglitz et al.*, 1999b].

[32] Today the transport of the Gulf Stream increases due to recirculation from approximately 30 Sv (Sverdrup = 10^6 m^3 s^{-1}) [*Schmitz and McCartney*, 1993] at the Florida Strait to somewhere between 50 $\sim$ 65 Sv [*Richardson and Knauss*, 1971; *Richardson*, 1977] and 90 Sv [*Halkin and Rossby*, 1985] near Cape Hatteras. If, during LGM, recirculation contributed significantly to the Gulf Stream transport in a manner similar to today, then the 10 Sv or so decrease in transport [*Lynch-Stieglitz et al.*, 1999b] at the Florida Strait may not substantially reduce the total Gulf Stream transport and thus inertia near Cape Hatteras. If so, the separation theory of inertial overshooting may still have the Gulf Stream separate at Cape Hatteras, consistent with our results. However, the assumption that the recirculation remained largely unchanged despite a one-third reduction

in transport at the Florida Straits may not be justified, given the inertial character of recirculation. If recirculation were also reduced by one third, the Gulf Stream would have been significantly weaker and may not have had sufficient energy for inertial overshooting. In this case, our reconstruction can be interpreted against the hypothesis of inertial overshooting.

[33] Another aspect of the ocean basin geometry that is possibly related to the Gulf Stream separation is bottom topography. Topographic control of the separation is supported by observations that the time-mean path of the Gulf Stream is fixed at two locations where distinct bathymetric features exist. One is New England Seamount Chain, and the other is Cape Hatteras where the continental slope is very steep: water depth changes by 2000 m in a horizontal distance of only about 20 km. Although the observations suggest a causal relationship, the dynamics of how a sudden step in topography affects the separation is not clear [*Dengg et al.*, 1996]. Simple consideration of the conservation of potential vorticity fails because it would require that the Gulf Stream turns poleward and follow the shelf break at Cape Hatteras to compensate for the sudden increase in water depth. Whatever the actual mechanism, if bottom topography steers the Gulf Stream away from the coast today, it should do likewise during LGM. This assumes that water column stratification remained unchanged, because it is the barotropic component of the current that ''feels'' the bottom. The effect of lowered LGM sea level by approximately 120 m [*Fairbanks*, 1989] is to make the Gulf Stream physically closer to bottom topography, so its control on separation if any would likely be enhanced.

[34] In addition to the Gulf Stream separation by (1) winds, (2) inertial overshooting, and (3) topographic changes, *Dengg et al.* [1996] classify major separation theories into three other groups: (4) detachment due to dynamically forced outcropping of isopycnal surfaces; (5) vorticity crisis; and (6) joint effect of baroclinicity and relief (JEBAR).

[35] The detachment prediction by isopycnal outcropping during LGM, like inertial overshooting, largely depends on the volume transport of the Gulf Stream. In this mechanism, first presented by *Parsons* [1969] and later expanded by *Veronis* [1973] and *Huang and Flierl* [1987], a northward increase of the meridional transport in the western boundary current would result by geostrophy in a corresponding northward increase of zonal gradient of the isopycnals. The increasingly steep isopycnals would eventually be forced to outcrop at the surface, which would then accomplish the current detachment from the coast. A weaker baroclinic transport of the LGM Gulf Stream at the Florida Strait [*Lynch-Stieglitz et al.*, 1999b] implies shallower isopycnal gradients, which would make it more difficult for isopycnals to outcrop and thus allow the Gulf Stream to separate further north by this mechanism. However, the weaker baroclinic transport of *Lynch-Stieglitz et al.* [1999b] is a result of shallow isopycnal gradients at depth, while the isopycnal gradients near the surface are relatively steeper. It is unclear to what extent this density structure at the Florida Strait will be maintained downstream.

[36] The central idea behind vorticity crisis is that there is a potential vorticity discontinuity between the western boundary and the Sverdrup interior. According to westward intensification theory, the subtropical gyre takes up negative vorticity from the winds over the eastern part of the basin that has to be dissipated by friction at the western boundary. However, the dissipation would be insufficient for highly inertial flow to remove the excess vorticity [*Pedlosky*, 1979], and the current experiences a ''vorticity crisis'' because it must dispose of this excess before being able to return to the low-vorticity interior. According to this theory, the Gulf Stream removes the vorticity excess by separating from the coast and setting up a region of intense vorticity transformation before reaching the interior. Since the separation depends on the nature of this highly nonlinear transformation, the effect of a larger vorticity input from stronger glacial winds is not at all predictable.

[37] The prediction is likewise unclear for JEBAR, which refers to the mathematical term containing potential energy of the density field and topography in the linearized vorticity equation for the vertically averaged flow [*Dengg et al.*, 1996]. Ocean circulation models that include this term are able to introduce the Northern Recirculation Region to the north of the separated Gulf Stream and south of Newfoundland (Figure 1), and the presence of the recirculation gyre apparently helps accurately depict the Gulf Stream separation. The recirculation actually consists in large part of the Deep Western Boundary Current (DWBC), which crosses underneath the Gulf Stream and continues southward along the continental slope. Prescribing the DWBC in some models brings simulations of Gulf Stream separation into slightly better but still limited agreement with observation [*Thompson and Schmitz*, 1989; *Gerdes and Köberle*, 1995]. Yet others have argued that the influence of JEBAR on the Gulf Stream is not from the depths of the DWBC but from the main thermocline [*Myers et al.*, 1996].

[38] These disagreements illustrate the complexity of JEBAR, and its effect on the Gulf Stream separation during LGM is unclear. We note however that the overturning of the Glacial North Atlantic Intermediate Water, which despite its name is approximately equivalent in depth to the modern upper North Atlantic Deep Water, may have been stronger during LGM [*Yu et al.*, 1996]. If the presence of DWBC is somehow important for the Gulf Stream separation as JEBAR suggests, a stronger DWBC underlying the Gulf Stream during LGM might be expected to influence the latitude of separation. Our results however do not indicate any such influence.

5. Conclusions

[39] The Gulf Stream today separates near Cape Hatteras from the coast and travels northeast as a free jet. The latitude of the separation coincides with the water mass boundary between the warm Gulf Stream and the cold Slope water and is well captured by the Holocene $\delta^{18}O$ of deep-dwelling planktonic foraminifera *G. truncatulinoides*. The glacial *G. truncatulinoides* $\delta^{18}O$ show that the Gulf Stream during the glacial time separated from the coast at nearly the same latitude as it does today. The reconstruction is consistent with the geometry of the ocean basin around Cape Hatteras, which remain unchanged over glacial-interglacial timescale, being the important control on the Gulf Stream separation. The likelihood of changes in glacial wind patterns

predicts changes in the separation latitude, making wind-forced separation less plausible. The effects of changes in the Gulf Stream baroclinicity and changes in DWBC on the latitude of separation are not entirely clear, so we cannot evaluate the plausibility of other theories with any certainty.

[40] **Acknowledgments.** We thank R. F. Anderson, A. J. Broccoli, J. Chiang, A. Gordon, and D. Pollard for discussions. L. Keigwin kindly provided sediment samples and oxygen isotope data. We also thank W. Balsam for making available carbonate data from his previous work. This research was supported with an NSF CAREER Award OCE 99-84989. Funding for radiocarbon dates was provided by a grants/cooperative agreement from the National Oceanic and Atmospheric Administration. The views expressed herein are those of the authors and do not necessarily reflect the views of NOAA or any of its subagencies. This is LDEO contribution number 6400.

References

Balsam, W., Late Quaternary sedimentation in the western North Atlantic: Stratigraphy and paleoceanography, *Paleogeogr. Paleoclimatol. Paleoecol.*, *35*, 215–240, 1981.

Bard, E., Correction of accelerator mass spectrometry ^{14}C ages measured in planktonic foraminifera: Paleoceanographic implications, *Paleoceanography*, *3*, 635–645, 1988.

Bartlein, P. J., K. H. Anderson, P. M. Anderson, M. E. Edwards, C. J. Mock, R. S. Thompson, R. S. Webb, T. Webb III, and C. Whitlock, Paleoclimate simulations for North America over the past 21,000 years: Features of the simulated climate and comparisons with paleoenvironmental data, *Quat. Sci. Rev.*, *17*, 549–585, 1998.

Bemis, B. E., H. J. Spero, J. Bijma, and D. W. Lea, Reevaluation of the oxygen isotopic composition of planktonic foraminifera: Experimental results and revised paleotemperature equations, *Paleoceanography*, *13*, 150–160, 1998.

Broccoli, A. J., Tropical cooling at the last glacial maximum: An atmosphere-mixed layer ocean model simulation, *J. Clim.*, *13*, 951–976, 2000.

Broecker, W. S., T.-H. Peng, S. Trumbore, G. Bonani, and W. Wolfi, The distribution of radiocarbon in the glacial ocean, *Global Biogeochem. Cycles*, *4*, 103–117, 1990.

Brunner, C. A., and P. E. Biscaye, Storm-driven transport of foraminifers from the shelf to the upper slope, southern Middle Atlantic Bight, *Cont. Shelf Res.*, *17*(5), 491–508, 1997.

Bush, A. B. G., and S. G. H. Philander, The climate of the last glacial maximum: Results from a coupled atmosphere-ocean general circulation model, *J. Geophys. Res.*, *104*, 24,509–24,525, 1999.

CLIMAP Project Members, Seasonal reconstructions of the Earth's surface at the Last Glacial Maximum, *Map Chart Serv. MC-36*, Geol. Soc. of Am., Boulder, Colo., 1981.

Dengg, J., A. Beckmann, and R. Gerdes, The Gulf Stream separation problem, in *The Warmwatersphere of the North Atlantic Ocean*, edited by W. Krauss, pp. 253–290, Gebrüder Borntraeger, Berlin, 1996.

Deuser, W. G., and E. H. Ross, Seasonally abundant planktonic foraminifera of the Sargasso Sea: Succession, deep-water fluxes, isotopic compositions, and paleoceanographic implications, *J. Foraminifera*, *19*(4), 268–293, 1989.

Fairbanks, R. G., A 17,000-year glacio-eustatic sea level record: Influence of glacial melting rates on the Younger Dryas event and deep-ocean circulation, *Nature*, *342*, 637–642, 1989.

Fairbanks, R. G., M. Sverdlove, R. Free, P. H. Wiebe, and A. W. H. Be, Vertical distribution and isotopic fractionation of living planktonic foraminifera from the Panama Basin, *Science*, *5877*, 841–843, 1982.

Fairbanks, R. G., C. D. Charles, and J. D. Wright, Origin of global meltwater pulses, in *Radiocarbon After Four Decades*, edited by R. E. Taylor, A. Long, and R. S. Kra, pp. 473–500, Springer-Verlag, New York, 1992.

Franklin, B., A letter from Dr. Benjamin Franklin, to Mr. Alphonsus le *R.* containing sundry maritime observations, *Trans. Am. Philos. Soc.*, *2*, 294–329, 1786.

Gangopadhyay, A., P. Cornillon, and D. R. Watts, A test of the Parsons-Veronis hypothesis on the separation of the Gulf Stream, *J. Phys. Oceanogr.*, *22*, 1286–1301, 1992.

Gates, W. L., Modeling the ice-age climate, *Science*, *191*, 1138–1144, 1976.

Gerdes, R., and C. Köberle, On the influence of DSOW in a numerical model of the North Atlantic general circulation, *J. Phys. Oceanogr.*, *25*, 2626–2642, 1995.

Halkin, D., and T. Rossby, The structure and transport of the Gulf Stream at 73°W, *J. Phys. Oceanogr.*, *15*, 1439–1452, 1985.

Hansen, D. V., Gulf Stream meanders between Cape Hatteras and the Grand Banks, *Deep Sea Res.*, *17*, 495–511, 1970.

Hemleben, C., M. Spindler, I. Breitinger, and W. G. Deuser, Field and laboratory studies on the ontogeny and ecology of some Globorotaliid species from the Sargasso Sea off Bermuda, *J. Foraminifera*, *15*(4), 254–272, 1985.

Horn, D. R., M. Ewing, B. M. Horn, and M. N. Delach, Turbidites of the Hatteras and Sohm Abyssal Plains, western North Atlantic, *Mar. Geol.*, *11*, 287–323, 1971.

Huang, R. X., and G. R. Flierl, Two layer models for the thermocline and current structure in the subtropical/subpolar gyres, *J. Phys. Oceanogr.*, *17*, 872–884, 1987.

Isemer, H. J., and L. Hasse, *The Bunker Climate Atlas of the North Atlantic Ocean*, 255 pp., Springer-Verlag, New York, 1987.

Keigwin, L. D., and G. A. Jones, Glacial-Holocene stratigraphy, chronology, and paleoceanographic observations on some North Atlantic sediment drifts, *Deep Sea Res.*, *36*, 845–867, 1989.

Kim, S.-T., and J. R. O'Neil, Equilibrium and nonequilibrium oxygen isotope effects in synthetic carbonates, *Geochim. Cosmochim. Acta*, *61*, 3461–3475, 1997.

Kutzbach, J. E., and P. J. Guetter, The influence of changing orbital parameters and surface boundary conditions on climate simulations for the past 18000 years, *J. Atmos. Sci.*, *43*(16), 1726–1759, 1986.

Kutzbach, J. E., R. Gallimore, S. Harrison, P. Behling, R. Selin, and F. Laarif, Climate and biome simulations for the past 21,000 years, *Quat. Sci. Rev.*, *17*, 473–506, 1998.

Ledbetter, M. T., and W. Balsam, Paleoceanography of the deep western boundary undercurrent on the North American continental margin for the past 25000 years, *Geology*, *13*, 181–184, 1985.

Levitus, S., and T. P. Boyer, *World Ocean Atlas 1994*, vol. 4, *Temperature*, *NOAA Atlas NESDIS 4*, 129 pp., Natl. Oceanic and Atmos. Admin., Silver Spring, Md., 1994.

Levitus, S., R. Burgett, and T. P. Boyer, *World Ocean Atlas 1994*, vol. 3, *Salinity*, *NOAA Atlas NESDIS 3*, 111 pp., Natl. Oceanic and Atmos. Admin., Silver Spring, Md., 1994.

Lohmann, G. P., and P. N. Schweitzer, *Globorotalia truncatulinoides*' growth and chemistry as probes of the past thermocline: 1. Shell size, *Paleoceanography*, *5*, 55–75, 1990.

Lynch-Stieglitz, J., W. B. Curry, and N. C. Slowey, A geostrophic transport estimate for the Florida Current from the oxygen isotope composition of benthic foraminifera, *Paleoceanography*, *14*, 360–373, 1999a.

Lynch-Stieglitz, J., W. B. Curry, and N. C. Slowey, Weaker Gulf Stream in the Florida Straits during the last glacial maximum, *Nature*, *402*, 644–648, 1999b.

Mulitza, S., A. Durkoop, W. Hale, G. Wefer, and H. Niebler, Planktonic foraminifera as recorders of past surface-water stratification, *Geology*, *25*, 335–338, 1997.

Munk, W. H., On the wind-driven ocean circulation, *J. Meteorol.*, *7*, 78–93, 1950.

Myers, R. A., and K. Drinkwater, The influence of Gulf Stream warm core rings on recruitment of fish in the northwest Atlantic, *J. Mar. Res.*, *47*, 635–656, 1989.

Myers, P. G., A. F. Fanning, and A. J. Weaver, JEBAR, bottom pressure torque, and Gulf Stream separation, *J. Phys. Oceanogr.*, *26*, 671–683, 1996.

Parsons, A. T., A two-layer model of Gulf Stream separation, *J. Fluid Mech.*, *39*, 511–528, 1969.

Pedlosky, J., *Geophysical Fluid Dynamics*, 624 pp., Springer-Verlag, New York, 1979.

Peltier, W. R., Ice age topography, *Science*, *265*, 195–201, 1994.

Pollard, D., and S. L. Thompson, Climate and ice-sheet mass balance at the last glacial maximum from the Genesis version 2 global climate model, *Quat. Sci. Rev.*, *16*, 841–863, 1997.

Ramstein, G., and S. Joussaume, Sensitivity experiments to sea surface temperatures, sea-ice extent and ice-sheet reconstruction, for the Last Glacial Maximum, *Ann. Glaciol.*, *21*, 343–347, 1995.

Rhines, P. B., and R. Schopp, The wind-driven circulation: Quasi-geostrophic simulations and theory for nonsymmetric winds, *J. Phys. Oceanogr.*, *21*, 1438–1469, 1991.

Richardson, P. L., On the crossover between the Gulf Stream and western boundary undercurrent, *Deep Sea Res.*, *24*, 139–159, 1977.

Richardson, P. L., and J. A. Knauss, Gulf Stream and western boundary undercurrent observations at Cape Hatteras, *Deep Sea Res.*, *18*, 1089–1109, 1971.

Schmitz, W. J., Jr., and M. S. McCartney, On the North Atlantic circulation, *Rev. Geophys.*, *31*, 29–49, 1993.

Schrag, D. P., and D. J. DePaolo, Determination of $\delta^{18}O$ of seawater in the deep ocean during the Last Glacial Maximum, *Paleoceanography*, *8*, 1–6, 1993.

Schrag, D. P., G. Hampt, and D. W. Murray, Pore fluid constraints on the temperature and oxygen isotopic composition of the glacial ocean, *Science*, *272*, 1930–1932, 1996.

Stanley, D. J., H. Sheng, and C. P. Pedraza, Lower continental rise east of the Mid-Atlantic States: Predominant sediment dispersal perpendicular to isobaths, *Geol. Soc. Am. Bull.*, *82*, 1831–1840, 1971.

Stommel, H., The westward intensification of wind-driven ocean currents, *Eos Trans. AGU*, *29*, 202–206, 1948.

Stommel, H., The Gulf Stream: A brief history of the ideas concerning its cause, *Sci. Monthly*, *70*(4), 242–253, 1950.

Taylor, A. H., and J. A. Stephens, The North Atlantic Oscillation and the latitude of the Gulf Stream, *Tellus, Ser. A*, *50*, 134–142, 1998.

Taylor, A. H., M. B. Jordan, and J. A. Stephens, Gulf Stream shifts following ENSO events, *Nature*, *393*, 638, 1998.

Thompson, L., and J. W. J. Schmitz, A limited-area model of the Gulf Stream: Design, initial experiments, and model-data intercomparison, *J. Phys. Oceanogr.*, *19*, 791–814, 1989.

Veronis, G., Model of the world ocean circulation: I. Wind-driven, two layer, *J. Mar. Res.*, *31*, 228–288, 1973.

Yu, E.-F., R. Francois, and M. Bacon, Similar rates of modern and last-glacial ocean thermohaline circulation inferred from radiochemical data, *Nature*, *379*, 689–694, 1996.

J. Lynch-Stieglitz, Lamont-Doherty Earth Observatory, P.O. Box 1000, Palisades, NY 10964, USA. (jean@ldeo.columbia.edu)

K. Matsumoto, Geological Survey of Japan, AIST Site 7, 1-1-1 Higashi, Tsukuba, Ibaraki 305-8567, Japan. (katsumi@ni.aist.go.jp)